

# Formation of Dopamine Adducts Derived from Brain Polyunsaturated Fatty Acids

## MECHANISM FOR PARKINSON DISEASE<sup>\*[5]</sup>

Received for publication, July 24, 2008, and in revised form, October 8, 2008 Published, JBC Papers in Press, October 15, 2008, DOI 10.1074/jbc.M805682200

Xuebo Liu<sup>†1</sup>, Naruomi Yamada<sup>†1</sup>, Wakako Maruyama<sup>§</sup>, and Toshihiko Osawa<sup>‡2</sup>

From the <sup>†</sup>Laboratory of Food and Biodynamics, Graduate School of Bioagricultural Science, Nagoya University, Nagoya 464-8601, Japan and the <sup>§</sup>Department of Basic Gerontology, National Institute for Longevity Science, Obu 474-8522, Japan

Oxidative stress appears to be directly involved in the pathogenesis of the neurodegeneration of dopaminergic systems in Parkinson disease. In this study, we formed four dopamine modification adducts derived from docosahexaenoic acid (C22:6/ $\omega$ -3) and arachidonic acid (C18:4/ $\omega$ -6), which are known as the major polyunsaturated fatty acids in the brain. Upon incubation of dopamine with fatty acid hydroperoxides and an *in vivo* experiment using rat brain tissue, all four dopamine adducts were detected. Furthermore, hexanoyl dopamine (HED), an arachidonic acid-derived adduct, caused severe cytotoxicity in human dopaminergic neuroblastoma SH-SY5Y cells, whereas the other adducts were only slightly affected. The HED-induced cell death was found to include apoptosis, which also seems to be mediated by reactive oxygen species generation and mitochondrial abnormality. Additionally, the experiments using monoamine transporter inhibitor and mouse embryonic fibroblast NIH-3T3 cells that lack the monoamine transporter indicate that the HED-induced cytotoxicity might specially occur in the neuronal cells. These data suggest that the formation of the docosahexaenoic acid- and arachidonic acid-derived dopamine adducts *in vitro* and *in vivo*, and HED, the arachidonic acid-derived dopamine modification adduct, which caused selective cytotoxicity of neuronal cells, may indicate a novel mechanism responsible for the pathogenesis in Parkinson disease.

Parkinson disease (PD)<sup>3</sup> is a neurodegenerative disorder characterized by a dramatic loss of dopaminergic neurons in

the substantia nigra and the subsequent deficiency of dopamine in the brain areas (1). Until now, very little is known about why and how the PD neurodegenerative process begins and progresses; however, an increasing body of evidence suggests that oxidative stress, mitochondrial dysfunction, and impairment of the ubiquitin-proteasome system may be involved in the pathogenesis of PD (2–5). Recent studies indicate that there are high levels of basal oxidative stress in the substantia nigra pars compacta in the normal brain, and this is increased in PD (6).

Oxidative stress in the brain easily leads to the lipid peroxidation reaction because of a high concentration of polyunsaturated fatty acids, such as docosahexaenoic acid (DHA, C22:6/ $\omega$ -3) and arachidonic acid (AA, C18:4/ $\omega$ -6), which are present in the brain (7). The polyunsaturated fatty acids are located almost exclusively in the SN2 position of the phosphoglycerides found in the neural cell membranes. The beneficial physiological effects of DHA and AA have been frequently reported (8, 9); however, the fatty acids are highly unsaturated, thus making them particularly susceptible to peroxidation. During the lipid peroxidation reaction, lipid hydroperoxides are generated as primary products. Subsequent decomposition leads to the formation of reactive mediators including aldehydes, which can covalently modify biomolecules. We have recently found that lipid hydroperoxides, the primary peroxidative products, can universally react with primary amino groups to form *N*-acyl-type (amide linkage) adducts (10–15). In our previous studies, the formation of linoleic acid-derived lysine modification adducts, *N*<sup>ε</sup>-(hexanoyl) lysine and *N*<sup>ε</sup>-(azelaoyl) lysine, and DHA-derived adducts, *N*<sup>ε</sup>-(succinyl) lysine and *N*<sup>ε</sup>-(propanoyl) lysine, have been identified *in vitro* or *in vivo* by liquid chromatography-MS/MS or immunochemical analysis. In addition, the formation of *N*<sup>ε</sup>-(hexanoyl) lysine also was detected, as well as *N*<sup>ε</sup>-(glutaryl) lysine, during the reaction of oxidized AA with the lysine residue. The *N*-acyl-type adducts are specific to the peroxidation of polyunsaturated fatty acids; therefore, their formations are useful markers for the lipid peroxidation, protein modification, and related dysfunction that occur in these fatty acid-enriched tissues.

Dopamine is the endogenous neurotransmitter produced by nigral neurons. Dopamine loss can trigger not only prominent secondary morphological changes, such as density reduction of the dendritic spines, but also changes in the density and sensitivity of dopamine receptors (1); therefore, it is a sign of PD development. The reasons for dopamine loss are attributed to

<sup>\*</sup> The costs of publication of this article were defrayed in part by the payment of page charges. This article must therefore be hereby marked "advertisement" in accordance with 18 U.S.C. Section 1734 solely to indicate this fact.

<sup>[5]</sup> The on-line version of this article (available at <http://www.jbc.org>) contains supplemental Figs. S1–S4.

<sup>†</sup> These authors contributed equally to this work.

<sup>‡</sup> To whom correspondence should be addressed: Furo-cho, Chikusa-ku, Nagoya 464-8601, Japan. Fax: 81-52-789-5741; E-mail: [osawat@agr.nagoya-u.ac.jp](mailto:osawat@agr.nagoya-u.ac.jp).

<sup>3</sup> The abbreviations used are: PD, Parkinson disease; DHA, docosahexaenoic acid; AA, arachidonic acid; SUD, succinyl dopamine; PRD, propanoyl dopamine; HED, hexanoyl dopamine; GLD, glutaroyl dopamine; NOD, nonanoyl dopamine; LAD, lauroyl dopamine; MTT, 3-(4,5-dimethylthiazol-2-yl)-2,5-diphenyltetrazolium bromide; PI, propidium iodide; PARP, poly(ADP-ribose) polymerase; 6-OHDA, 6-hydroperoxydopamine; ROS, reactive oxygen species; MS/MS, tandem mass spectrometry; HPLC, high performance liquid chromatography; FBS, fetal bovine serum; DMEM, Dulbecco's modified Eagle's medium; DCF, dichlorofluorescein; DAT, dopamine transporter; NET, norepinephrine transporter; 5-HTT, serotonin transporter; HEDOPA, hexanoyl dihydroxyphenylalanine.

the molecular instability of dopamine. Some possible causes of dopamine loss are abnormalities of dopaminergic neurons (16), dopamine degradation by monoamine oxidase A (17) or auto-oxidation (18) and the reaction with amino acid cysteine (19). Dopamine is a member of catecholamine family. The catechol structure contributes to high oxidative activation of dopamine. Additionally, the N termini in the structure of dopamine may represent another reactive spot; however, little experimental evidence proves this. Based on our previously described reaction between lipid hydroperoxides and N-terminal residues, we focused on the possibility that reactive hydroperoxide species derived from lipid peroxidation may modify dopamine to form amide linkage dopamine adducts.

In the present study, we chemically synthesized four dopamine-modified adducts derived from DHA and AA. We were particularly interested in the formation of the dopamine adducts by chemical reactions and *in vivo* experiments, as well as the cytotoxicity evaluation using neuronal cells. All four dopamine adducts were detected upon incubation of dopamine with fatty acid hydroperoxides and an *in vivo* experiment using rat brain tissue. Furthermore, we focused on an AA-derived adduct HED, which induced severe cytotoxicity in human dopaminergic neuroblastoma SH-SY5Y cells compared with other adducts. The HED-induced cell death was found to include apoptosis that might be mediated by reactive oxygen species (ROS) and mitochondrial abnormality in SH-SY5Y cells. In addition, we found that the presence of monoamine transporters in the cells was essential for the HED-induced cytotoxicity, suggesting the specificity of the cytotoxicity to the cells. Taken together, the DHA- and AA-derived dopamine adducts may be useful biomarkers of the dopamine deficiency, and the formation of these adducts may indicate a novel mechanism responsible for the pathogenesis in Parkinson disease.

## EXPERIMENTAL PROCEDURES

**Materials**—DHA, arachidonic acid, lipoxidase, GBR 12909 dihydrochloride, imipramine hydrochloride, *N*-acetyl-Asp-Glu-Aal-Asp-al, and RNase were obtained from Sigma-Aldrich (Tokyo, Japan). Dopamine·HCl was purchased from Nacalai Tesque, Inc. (Kyoto, Japan). Linoleic acid, hexanoic anhydride, glutaric anhydride, propanoic anhydride, succinic anhydride, lauric anhydride, and nonanoic anhydride were obtained from Wako Pure Chemical Industries, Ltd. (Osaka, Japan). The antibodies against cytochrome *c* oxidase IV and poly(ADP-ribose) polymerase (PARP) were purchased from Cell Signaling Technology, Inc. (Boston, MA). Active caspase-3 rabbit monoclonal antibody was purchased from Epitomics, Inc. (Burlingame, CA).

**Synthesis of *N*-Acyl Dopamine Adducts**—The *N*-acyl dopamine adducts were chemically synthesized by incubating dopamine (0.5 mM) with carboxylic or methylic anhydride (0.5 mM) in 5 ml of 100 mM sodium phosphate buffer (pH 7.4)-saturated sodium acetate (1:1, v/v) for 60 min at room temperature. Succinic anhydride and propanoic anhydride were utilized for preparing the succinyl dopamine (SUD) and propanoyl dopamine (PRD), respectively; Hexanoic anhydride and glutaric anhydride were used for synthesizing the HED and glutaroyl dopamine (GLD), respectively. The synthesized adducts were purified by reverse phase HPLC using a Develosil ODS-HG-5

column (20 × 250 mm) in an isocratic system of 15 or 50% acetonitrile containing 0.1% trifluoroacetic acid at the flow rate of 6 ml/min. The elution profiles were monitored by absorbance at 280 nm. The amino residues in the dopamine adducts were identified by the ninhydrin reaction. The mass, structure, and formula of the synthesized molecule were identified by HPLC-MS, NMR, and electrospray ionization time-of-flight mass spectrometry analyses, respectively.

**HPLC-Tandem Mass Spectrometry**—The HPLC-MS/MS analysis was carried out using an API 2000 triple quadrupole mass spectrometer (Applied Biosystems) through a Turbolon-Spray source. Chromatography was carried out on a Develosil ODS-HG-3 column (2.0 × 250 mm) using an Agilent 1100 HPLC system. The chromatographic separation was performed by a gradient elution as follows: 0–10 min, linear gradient from 0.1% formic acid to 50% aqueous acetonitrile containing 0.1% formic acid; 10–15 min, hold; 15–20 min, linear gradient to 0.1% formic acid; flow rate = 0.2 ml/min. The instrument response was optimized by infusion experiments with the standard compounds using a syringe pump at the flow rate of 5  $\mu$ l/min. The dopamine adducts were detected using electrospray ionization MS/MS in the multiple reaction monitoring mode.

**In Vitro Modification of Dopamine**—DHA hydroperoxides were prepared from the DHA auto-oxidative reaction, and AA hydroperoxides were prepared using 15-lipoxygenase. The levels of lipid hydroperoxide were determined using a lipid hydroperoxide assay kit (Cayman Chemical Co., Ann Arbor, Michigan). Dopamine (2 mM) was incubated with 10 mM of DHA or AA hydroperoxides in phosphate buffer (pH 7.4) at 37 °C for different times. The reaction was terminated by immediate freezing at –80 °C. AA hydroperoxide was prepared as described previously (11).

**In Vivo Detection of Dopamine Adducts**—Brain homogenates of 7- and 27-week-old male F344/NSIc rats were used to detect the dopamine adducts. Briefly, the rat brain was removed and homogenized with phosphate-buffered saline containing 5% dibutylhydroxytoluene (5 mM) and EDTA (250 mM). After the addition of the deuterated dopamine adducts (20  $\mu$ M) as the internal standard, the homogenates were centrifuged at 3,000 rpm for 10 min. The pellet was then dissolved in 100  $\mu$ l of methanol. The detection was carried out by HPLC-MS/MS.

**Cell Cultures and Drug Treatment Procedures**—SH-SY5Y human dopaminergic neuroblastoma cells and NIH-3T3 mouse embryonic fibroblast cells were kindly donated by Dr. Maruyama (National Institute for Longevity Science). SH-SY5Y cells and NIH-3T3 cells were grown in Cosmedium-001 (Cosmo-Bio, Tokyo, Japan) containing 5% FBS and DMEM containing 10% FBS, respectively, and maintained at 37 °C in an atmosphere of 5% CO<sub>2</sub> in air. The 80% confluent cells were allowed to medium change with FBS-free DMEM overnight. The dissolved drugs were diluted by 1/500 or 1/1000 and added to fresh FBS-free DMEM to achieve the required concentration.

**Assessment of Cell Viability**—Cell viability was evaluated by an MTT assay. SH-SY5Y cells in 96-well plates were incubated with drugs for different times, followed by further incubation with 500  $\mu$ g/ml MTT at 37 °C for 2 h. Cell viability in some experiments was also measured using PI and Hoechst 33258 staining.

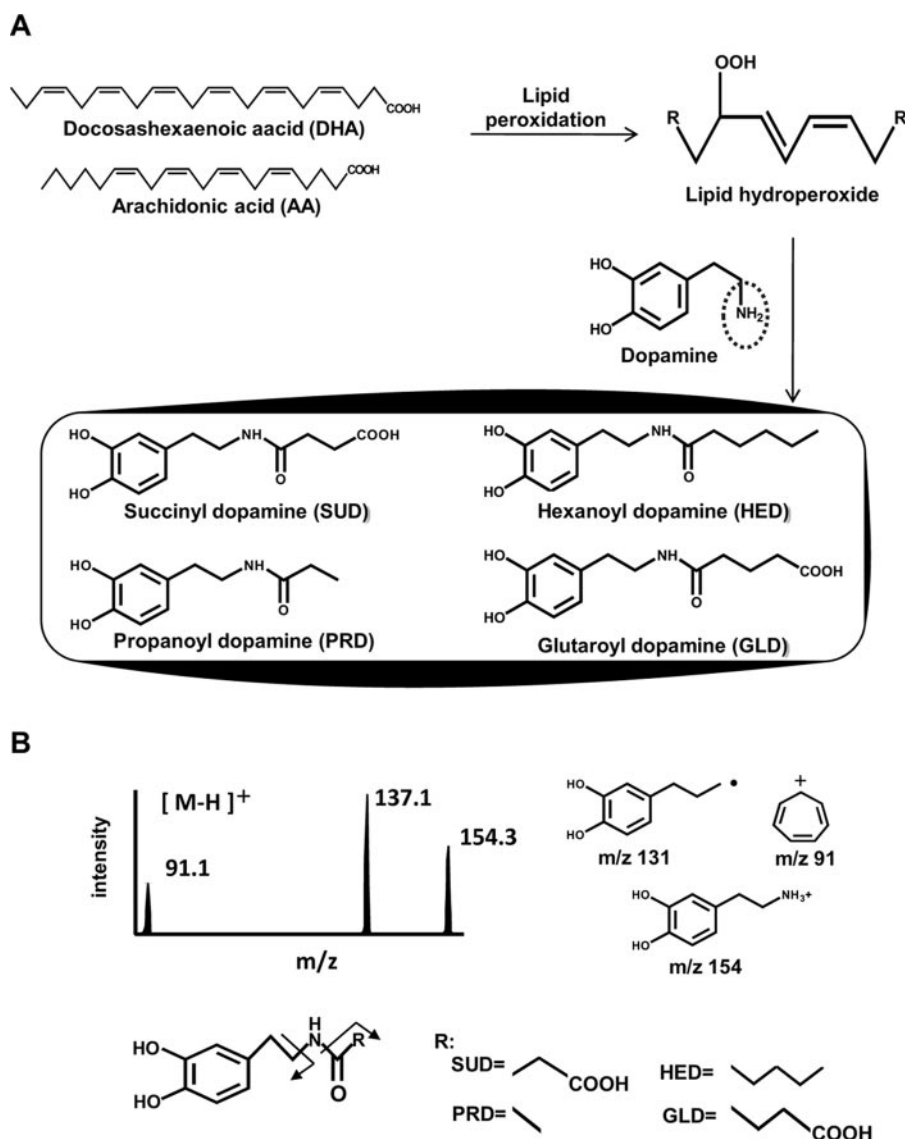


**FIGURE 1. Proposed chemical formation scheme and HPLC-MS/MS analysis of DHA- and AA-derived dopamine adducts.** A, proposed reaction scheme of DHA- and AA-derived dopamine adduct formation. B, the  $[MH]^+$  ion  $m/z$  254, 210, 252, and 268 of SUD, PRD, HED, and GLD, respectively, were subjected to collision-induced dissociation, and the daughter ions were scanned (upper left panel). The proposed structures of individual ions are shown (upper right panel). The chemical structure composition of the dopamine adducts is proposed by fragmental analysis (lower panel).

**ROS Measurement**—Endogenous ROS level was detected by flow cytometry using  $H_2DCF$ -DA (2',7',-dichlorodihydrofluorescein diacetate) (Molecular Probes). Briefly, the drug-treated cells were incubated with  $H_2DCF$ -DA for 30 min, and the fluorescence of dichlorofluorescein (DCF) was measured using an EPICS Elite Flow Cytometer.

**DNA Fragmentation Assay**—The drug-treated SH-SY5Y cells were collected, suspended in 0.2 ml of lysis buffer (20 mM Tris-HCl, pH 7.5, 10 mM EDTA, and 0.5% Triton X-100), and incubated at room temperature for 10 min. The samples were then centrifuged at  $12,000 \times g$  for 10 min, and the supernatant containing the DNA cleavage products was incubated with 0.2 mg/ml proteinase K at  $37^\circ C$  for 1 h followed by 0.1 mg/ml RNase A for 30 min at  $50^\circ C$ . The DNA fragments were purified by phenol/chloroform extraction and ethanol precipitation and

then separated on an ethidium bromide (0.5 mg/ml)-containing 2% agarose gel.

**Subcellular Fraction of SH-SY5Y Cell**—The cells are harvested by centrifugation at  $600 \times g$  for 10 min, washed with phosphate-buffered saline, and resuspended with 5 volumes of Solution A (0.25 M sucrose, 20 mM HEPES-KOH, pH 7.5, 10 mM KCl, 1.5 mM  $MgCl_2$ , 1 mM EDTA, 1 mM EGTA, 1 mM dithiothreitol, 0.1 mM phenylmethylsulfonyl fluoride). The cellular suspension was homogenized with a glass-glass homogenizer with 20 up and down passes of the pestle. The homogenate was then centrifuged at  $750 \times g$  for 10 min. The resulting supernatant was collected and then centrifuged at  $10,000 \times g$  for 15 min. The pellet was used as the mitochondrial fraction.

**Western Blot Analysis**—The cells were washed twice with phosphate-buffered saline, pH 7.0, and lysed with lysis buffer (50 mM Tris-HCl, pH 7.5, 150 mM NaCl, 1% Triton X-100, 0.5% sodium deoxycholate, 0.1% SDS, 100  $\mu g/ml$  phenylmethylsulfonyl fluoride). After protein quantification, equal amounts of the protein (total protein, 20–50  $\mu g$ ) were boiled with Laemmli sample buffer for 5 min at  $100^\circ C$ . The samples were run on 10% SDS-polyacrylamide gels, transferred to a nitrocellulose membrane, incubated with 5% skim milk in TTBS (Tris-buffered saline containing 10% Tween 20) for blocking, washed, and treated with the primary antibodies. After washing with TTBS, the blots were further incubated for

1 h at room temperature with the IgG antibody coupled to horseradish peroxidase in TTBS. The blots were then washed three times in TTBS before visualization. An ECL kit was used for detection.

**Statistical Analysis**—All of the data were analyzed using Bonferroni/Dunn's multiple comparison procedure.

## RESULTS

**Chemical Formation of DHA- and AA-derived Dopamine Adducts**—Based on the observations that lipid hydroperoxides, the primary products of lipid peroxidation, could universally react with primary amino groups to form *N*-acyl-type (amide linkage) adducts, and also within the chemical structure of dopamine, an amino residue is present, we chemically synthesized the four amide linkage dopamine adducts, SUD, PRD, HED,



## DHA- and AA-derived Dopamine Adducts

and GLD, that were derived from DHA and AA, respectively (Fig. 1A). The chemical structures of the authentic adducts were identified by NMR (supplemental Figs. S1–S4). The formation of these dopamine adducts was further confirmed by HPLC-MS/MS analysis. Collision-induced dissociation of the authentic adducts SUD ( $m/z$  254), PRD ( $m/z$  210), HED ( $m/z$  252), and GLD ( $m/z$  268) produced the same daughter ions at  $m/z$  91 and 137. SUD, PRD, and HED also produced daughter ions at  $m/z$  154, whereas GLD did not. These ions were assigned the structures shown in Fig. 1B. The ion at  $m/z$  137 was detected with the highest peak intensity in the fragments, and this ion was also identified to be derived from the dopamine spectra.

**In Vitro Detection of Dopamine Adducts**—To determine the *in vitro* formation of the dopamine adducts, the reaction of dopamine with DHA or AA hydroperoxides were carried out. The reaction mixture was analyzed by HPLC-MS/MS based on the information in the collision-induced dissociation spectra. As shown in Fig. 2, the peaks indicating SUD, PRD, HED, and GLD were successfully detected at  $m/z$  254  $\rightarrow$  137,  $m/z$  210  $\rightarrow$  137,  $m/z$  252  $\rightarrow$  137, and  $m/z$  268  $\rightarrow$  137, respectively. The retention times were consistent with those of the authentic adducts.

**In Vivo Detection of Dopamine Adducts**—It has been reported that polyunsaturated fatty acids such as DHA and AA are significantly enriched in the brain (20) and that there are high levels of basal oxidative stress in the normal brain, which increases with aging (21). To investigate whether the DHA- and AA-derived dopamine adducts can be formed *in vivo*, the brains of 7- and 27-week-old male F344/NSlc rats were removed, and the homogenates were used. The detection of the dopamine adducts in the homogenates was carried out by HPLC-MS/MS. The whole adducts were detected in the 7- and 27-week rat brains in both the positive ion mode and negative ion mode of liquid chromatography-MS/MS (data not shown). The level of adduct formation was shown in Fig. 3. The HED and PRD, which are derived from the C terminus of AA and DHA, were more significantly formed than SUD and PRD; however, no significant difference of adduct level was found between the 7- and 27-week-old rats.

**Identification of HED as a Potent Inducer of Neuronal Apoptosis**—In recent years, several dopamine oxidants and dopamine-modified adducts have been reported, such as neuromelanin (22), aminochrome (23), 6-OHDA (24), and 5-S-synthindopamine (19), in which 6-OHDA has been generally known as a potent neurotoxin (25–27). We hypothesized that some of these DHA- and AA-derived dopamine adducts could cause neuronal cell death. To test this hypothesis, the effect of these dopamine adducts on the cell viability in SH-SY5Y cells was studied. After treatment with 100  $\mu$ M of the sample for 24 h, among the tested dopamine adducts, HED and PRD induced about 80 and 30% of the cell death, respectively. On the other hand, SUD and GLD had almost no influence on the cell viability (Fig. 4A), suggesting that the death of SH-SY5Y cells was induced only by the C terminus-derived adducts and not by the C terminus-derived adducts. Of interest, two HED analogs, nonanoyl dopamine (NOD) and lauroyl dopamine (LAD), which were synthesized in this study and characterized by more carbons than HED in the methyl terminus, also showed

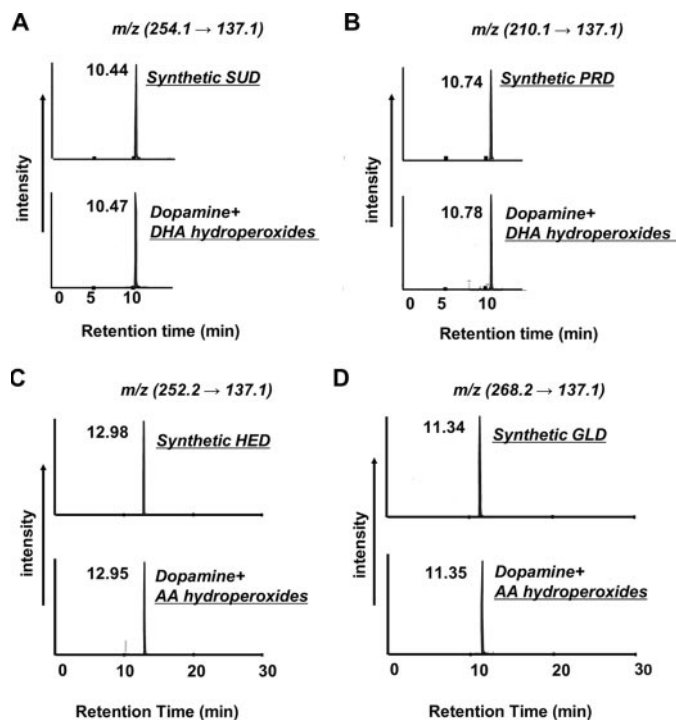


**FIGURE 2. HPLC-MS/MS analysis of the dopamine adducts formed during the reaction of dopamine with oxidized DHA and AA hydroperoxides.** Dopamine (2 mM) was incubated with lipid hydroperoxides (10 mM) in 0.1 M phosphate buffer (pH 7.4) at 37 °C. Shown is selected ion monitoring of the transitions from  $m/z$  254 (A), 210 (B), 252 (C), and 268 (D) to  $m/z$  137 for SUD, PRD, HED, and GLD, respectively. Top panels, authentic dopamine adduct; bottom panels, reaction mixture of DHA- or AA hydroperoxides with dopamine.

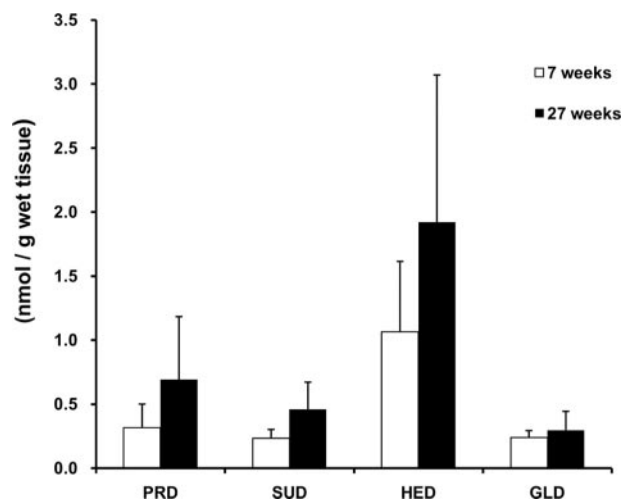


**FIGURE 3. Formation of the dopamine adducts *in vivo*.** The levels of dopamine adduct formed in rat brain were determined by HPLC-MS/MS (data are shown as the means  $\pm$  S.D. ( $n = 5$ )).

a significant toxicity to SH-SY5Y cells (Fig. 4B), suggesting that the number of carbons in the C terminus-derived dopamine adducts might be associated with the adduct-induced cell death.

Remarkably, HED was a potent inducer of SH-SY5Y cell death compared with SUD, PRD, and GLD. Because the main cause of neuronal cell death has been postulated to be apoptosis, we then characterized whether HED-induced cell death in SH-SY5Y cells includes apoptosis. As shown in Fig. 5A, the

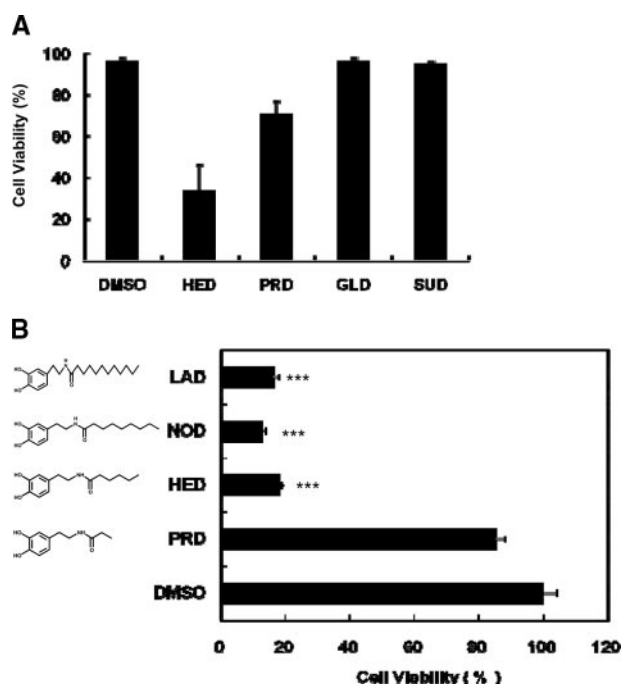


**FIGURE 4. Identification of HED as a potent inducer of cell death in SH-SY5Y cells.** The cells were exposed to 100  $\mu$ M sample for 24 h. Cell viability was measured by the MTT assay. In the MTT assay, the data are expressed as percentages of control culture conditions. *A*, potential comparison of cell death induction by DHA- and AA-derived dopamine adducts. *B*, effect of carbon numbers in C terminus in the structure of dopamine-derived adducts to cell viability in the cells (data are shown as the means  $\pm$  S.D. ( $n = 3$ ); \*\*\*, indicates  $p < 0.001$ ).

exposure to HED led to a dose-dependent decrease in the viable cells. When the SH-SY5Y cells were exposed to 10  $\mu$ M HED for 4 h, the fragmented nuclei were found in cells exhibiting the typical morphological features of apoptosis (Fig. 5B). In addition, the gel electrophoresis of DNA from the SH-SY5Y cells exposed to HED also displayed nucleosomal DNA fragmentation (Fig. 5C). HED treatment also led to the time- and dose-dependent cleavage of PARP, resulting in the accumulation of the 85-kDa fragment and decreasing in the 116-kDa protein, as well as in the accumulation of the active caspase-3 (Fig. 5D), both of which are hallmarks of apoptosis. Moreover, the pretreatment with the caspase-3 inhibitor significantly prevented SH-SY5Y cells from HED-induced DNA fragmentation (Fig. 5E), providing further evidence that HED induced a caspase-3-mediated apoptotic cell death.

**Regulation of HED-induced Apoptosis in SH-SY5Y Cells**—We next investigated the signaling mechanism underlying the HED-induced apoptosis. It is well accepted that ROS generation is a key contributor to neuronal apoptosis induced by neurotoxin compounds (28). Hence, experiments were first carried out to assess ROS generation induced by the HED treatment and the possibility that the HED-induced apoptosis is mediated via ROS generation in SH-SY5Y cells. As shown in Fig. 6A, HED led to about a 3.5-fold increased ROS generation in the cells compared with the Me<sub>2</sub>SO-treated cells, whereas the other three dopamine adducts, SUD, PRD, and GLD, had much less of an effect on the cells. Furthermore, after the HED treatment for 30 min, a dose-dependent increase in ROS generation was found by DCF fluorescence staining (Fig. 6B). The pretreatment

with *N*-acetyl-L-cysteine, a potent antioxidant, clearly inhibited the PARP cleavage (Fig. 6C), indicating that ROS generation might be critically involved in the HED-induced apoptosis.

It is widely accepted that mitochondrial dysfunction may play very important roles in neuronal cell death (29). Here, we examined cytochrome *c* release from mitochondria in the cells, which are an important feature of mitochondrial change and a potent inducer of caspase-3 activation. As shown in Fig. 6D, dose- and time-dependent decreases of cytochrome *c* expression in the mitochondrial fraction were obviously observed in HED-treated cells.

**Effect of Monoamine Transporter Inhibition on HED-induced Apoptosis and ROS Generation**—Monoamine transporters including the dopamine transporter (DAT), norepinephrine transporter (NET), and 5-HT transporter (5-HTT), which are of fundamental importance for proper signaling between neurons, have been reported to associate with experimental neurotoxins-induced toxicity (30). HED possesses a dopamine-based chemical structure; therefore, in this study we hypothesized that the above-described HED cytotoxicity that occurred in the SH-SY5Y cells might be mediated by some monoamine transporters. To evaluate this hypothesis, we used the monoamine transporter inhibitor to investigate the effect of DAT, NET, and 5-HTT on HED-induced apoptosis and ROS generation. As shown in Fig. 7A, the pretreatment with both GBR12909 and imipramine, the inhibitors of DAT and NET/5-HTT, respectively, clearly inhibited the occurrence of the HED-induced PARP cleavage and active caspase-3 expression in the SH-SY5Y cells. Furthermore, ROS generation by HED was also found to be suppressed in these two inhibitor-pretreated cells. The result that both monoamine transporter inhibitors showed markedly inhibitive effect on the HED-induced apoptosis and ROS generation suggested that HED might be primarily transported into the SH-SY5Y cells by the monoamine transporters and inflicted damage on the cells.

**Influence of HED to NIH-3T3 Cell Lines**—To characterize whether the HED-induced cytotoxicity is specific to neuronal cells, we investigated the effect of HED on apoptotic cell death and ROS generation in mouse embryonic fibroblast NIH-3T3 cells in comparison with that of the SH-SY5Y cells. A dose-dependent analysis revealed that HED led to no apoptotic cell death in the NIH-3T3 cells based on Hoechst 33258 and PI nuclear staining (Fig. 8A). A further quantitative analysis of the apoptotic cells by flow cytometry also indicated a significant apoptosis in SH-SY5Y cells, whereas not in the NIH-3T3 cells (Fig. 8B). Moreover, no ROS generation was found in the HED-treated NIH-3T3 cells; on the other hand, the HED analogs, NOD and LAD, also induced only a slight ROS generation in the NIH-3T3 cells (Fig. 8C). These data and the fact that monoamine transporter is absent in NIH-3T3 cells suggest that the HED-induced cytotoxicity might be specific to neuronal cells.

## DISCUSSION

The nervous system is particularly vulnerable to the deleterious effect of ROS, and one of the main reasons is that the brain contains high concentrations of polyunsaturated fatty acid that are highly susceptible to lipid peroxidation (31, 32). In recent years, an increasing body of evidence suggests that oxidative

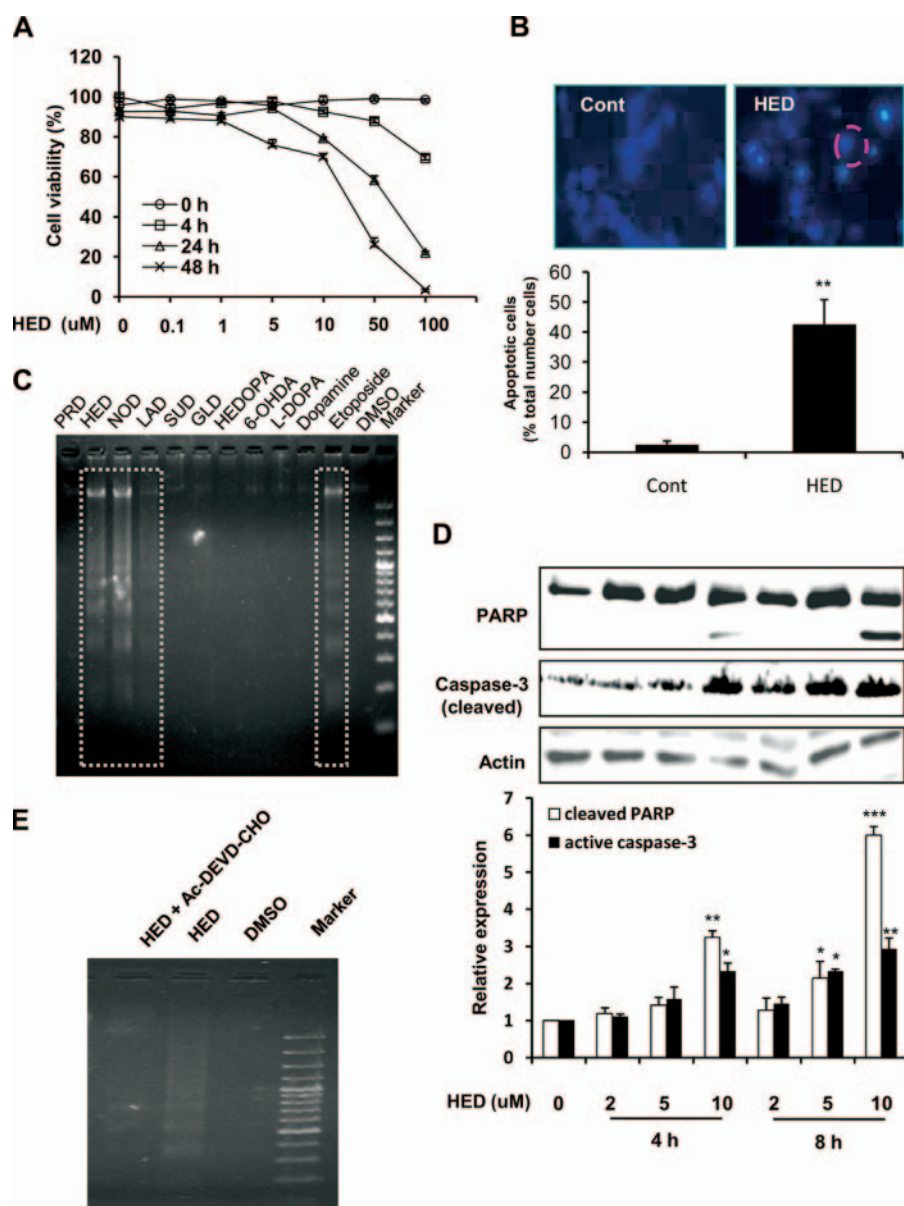


**FIGURE 5. Apoptosis induced by HED.** A, dose- and time-dependent cytotoxicity of HED. SH-SY5Y cells were exposed to 0–100  $\mu$ M HED for different retention times. Cell viability was measured by the MTT assay. B, chromatin condensation in SH-SY5Y cells exposed to 10  $\mu$ M HED. The cells were fixed with paraformaldehyde, stained with Hoechst 33258, and examined by fluorescence microscopy. Upper left panel, control (Cont) cells staining. Upper right panel, HED-treated cells staining. Lower graph, statistical analysis of apoptotic cells. C, DNA fragmentation in SH-SY5Y cells exposed to 25  $\mu$ M HED or other samples for 12 h. Nucleosomal DNA fragmentation was visualized by agarose gel electrophoresis. D, PARP cleavage and active caspase-3 expression in SH-SY5Y cells exposed to 0–10  $\mu$ M HED for 4 h and 8 h. The cleavage of PARP and expression of active caspase-3 were tested by Western blotting and statistically analyzed. E, effect of caspase-3 inhibitors on HED-induced DNA fragmentation. The inhibitor used was AC-DEVD-CHO. The SH-SY5Y cells were treated with 25  $\mu$ M HED for 12 h in the presence or absence of inhibitor for 30 min. DNA fragmentation was visualized by agarose gel electrophoresis. All of the data are shown as the means  $\pm$  S.D. ( $n = 3$ ) (significantly different from control: \* indicates  $p < 0.05$ , \*\* indicates  $p < 0.01$ , and \*\*\* indicates  $p < 0.001$ ).

stress is pathologically involved in neurodegenerative disorders (33) including PD and Alzheimer disease. It is also generally accepted that lipid peroxidation, a central feature of oxidative stress, is an important reaction leading to oxidative damage in biomolecules, such as DNA and proteins (34–36). In the present study, we determined the formation of brain polyunsaturated fatty acid-derived dopamine adducts *in vitro* and *in vivo*. We also found that HED, an AA-derived dopamine adduct,

significantly induced a monoamine transporter-mediated ROS generation and apoptosis in the SH-SY5Y cells. These data suggest that the DHA- and AA-derived dopamine adducts may be useful biomarkers, and their formation may be critically involved in the pathogenesis of Parkinson disease.

PD is one of the most common neurodegenerative disorders among the aged, and its pathological hallmark is the selective degeneration of dopaminergic neurons in the substantia nigra accompanied with the subsequent deficiency of dopamine in the brain areas. The etiology of PD remains unclear, but recently, mutation of the genes encoding  $\alpha$ -synuclein and parkin was linked with familial PD. Additionally, dysfunction of mitochondria complex 1 and increase in oxidation of biomolecules were detected in dopamine neurons of postmortem brains of patients with idiopathic PD (37, 38). Lipid peroxidation, the central feature of oxidative stress, has been shown to increase in the PD brain, which is shown by such occurrences as increased malondialdehyde levels (39), HNE-modified proteins (40) and cholesterol lipid hydroperoxide (41), and lipoprotein oxidation in cerebrospinal fluid and plasma (42).

The sources of lipid peroxidation in the brain are thought to mainly originate from the peroxidation of DHA and AA because of their high contents in the brain relative to other organs (43) and highly unsaturated properties. In our previous reports, we have described that DHA and AA hydroperoxide, the primary products of fatty acid peroxidation, can universally react with primary amino groups to form amide linkage adducts including  $N^\epsilon$ -(succinyl) lysine,  $N^\epsilon$ -(propanoyl) lysine,  $N^\epsilon$ -(hexanoyl) lysine, and

$N^\epsilon$ -(glutaryl) lysine; however, through this study it is now recognized that DHA and AA hydroperoxides can also modify dopamine by an *N*-acyl-type adduct-formed reaction (Fig. 1).

Dopamine is a natural neurotransmitter in the brain, and its deficiency is a sign of Parkinson disease (44). Although the reason for dopamine loss is not fully understood, some considerations include dopaminergic neuron abnormalities, dopamine degradation by monoamine oxidase A, and auto-oxidation and



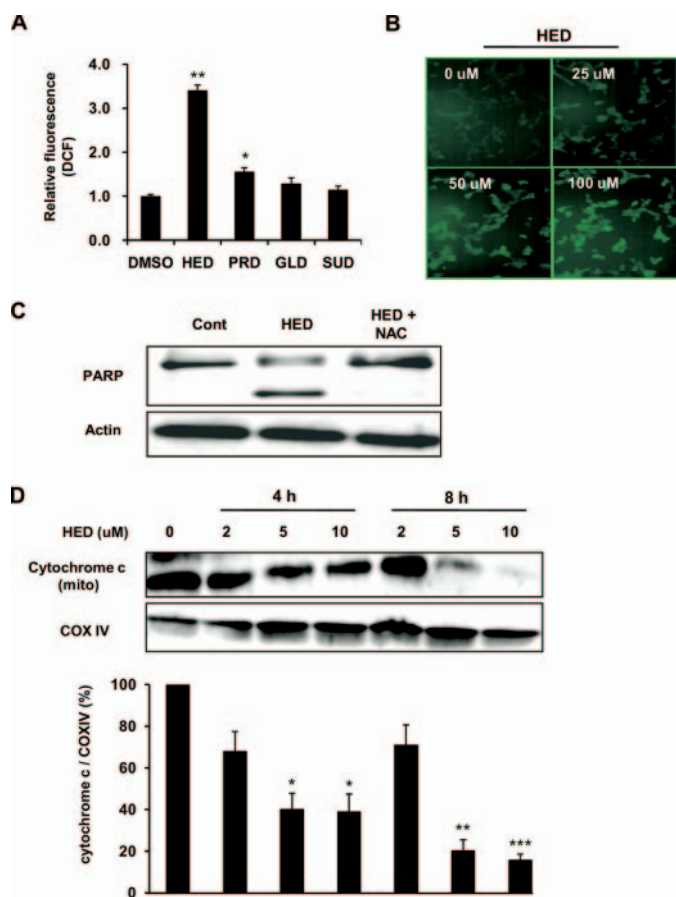


**FIGURE 6. ROS generation and cytochrome c release during HED-induced apoptosis.** *A*, comparison of ROS generation induced by DHA- and AA-derived dopamine adducts. The SH-SY5Y cells were treated with 10  $\mu$ M dopamine adducts for 30 min and exposed to H<sub>2</sub>DCF-DA for 30 min. The fluorescence of DCF was measured by flow cytometer. *B*, dose-dependent ROS generation induced by HED. DCF fluorescence imaging was determined by fluorescence microscope. *C*, effect of antioxidant *N*-acetyl-L-cysteine on HED-induced PARP cleavage and accumulation of active caspase-3. 50 mM *N*-acetyl-L-cysteine was administered in SH-SY5Y cells for 30 min before HED treatment. *D*, cytochrome c release induced by HED. The SH-SY5Y cells were treated with different concentrations of HED for 0, 4, and 8 h. The expressions of cytochrome c and cytochrome c oxidase IV (COX IV) in the mitochondrial fraction of HED-treated cells were assessed by Western blot. All of the data are shown as the means  $\pm$  S.D. ( $n = 3$ ) (significantly different from control: \* indicates  $p < 0.05$ , \*\* indicates  $p < 0.01$ , and \*\*\* indicates  $p < 0.001$ . DMSO, dimethyl sulfoxide; Cont, control).

modification (17–19). The *in vitro* and *in vivo* detections of DHA- and AA-derived dopamine adducts established in this study (Figs. 2 and 3) may indicate an additional clue to the causes of dopamine deficiency in PD. Although the level of the dopamine adducts was not obviously increased in the 27-week-old rat brain compared with the 7-week-old rat brain, 27 weeks represents only middle age for a rat, and the level of basal oxidative stress is increased with age (45–47); therefore, further study should confirm these adduct formations in the brain using aging model rats such as rats 1 year old and more and also PD model animals.

Dopamine-derived metabolites have been reported to inflict damage on neuronal cells (48). For example, 6-OHDA, a hydroxylated analog of dopamine, has been demonstrated to induce apoptosis in several neuronal cell lines (49–52). In addition, dopamine auto-oxidation generating dopamine quinone

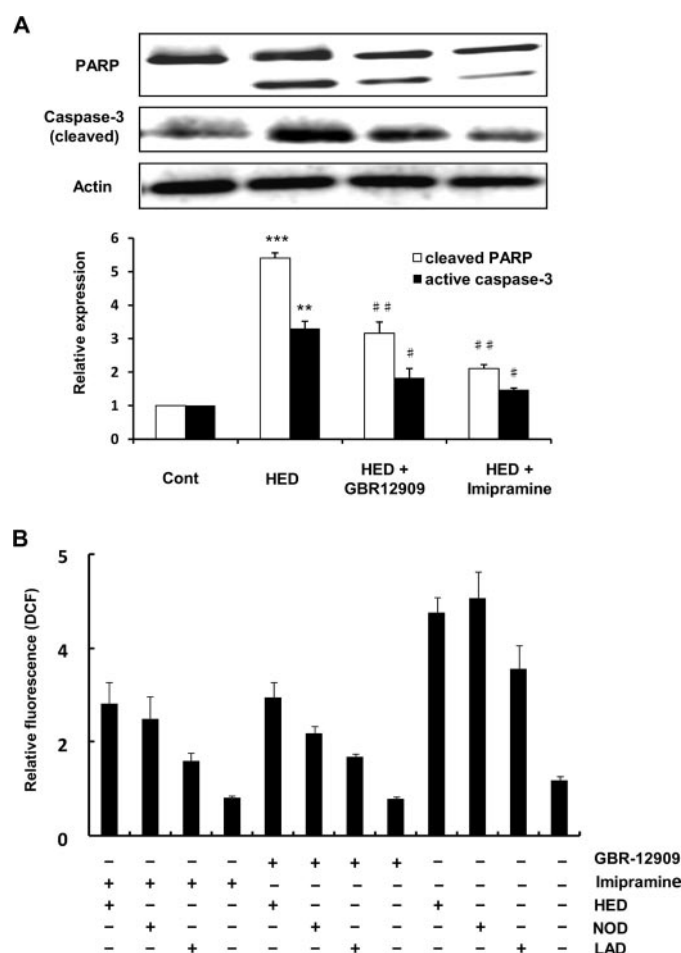


**FIGURE 7. Effect of monoamine transporter inhibitors on apoptosis and ROS generation.** The inhibitors used were GBR 12909 and imipramine for DAT and NET/5-HTT, respectively. 1  $\mu$ M inhibitors were administered in SH-SY5Y cells for 30 min before drug treatments. *A*, effect of monoamine transporter inhibitors on HED-induced PARP cleavage and accumulation of active caspase-3. Cleaved PARP and the expression of active caspase-3 were statistically analyzed. *B*, effect of monoamine transporter inhibitors on HED-induced and HED analog-induced ROS generation. All of the data are shown as the means  $\pm$  S.D. ( $n = 3$ ) (significantly different from control: \*\*\* indicates  $p < 0.001$ ; significantly different from HED alone: # indicates  $p < 0.05$ , and ## indicates  $p < 0.01$ ). Cont, control.

can react with protein sulfhydryl groups leading to structural modifications of proteins and reduced levels of glutathione (53). In the present study, we found that HED, an AA-derived dopamine adduct, caused significant cell death in SH-SY5Y cells (Fig. 4A). Furthermore, the events including DNA fragmentation, chromatin condensation, PARP cleavage, and accumulation of active caspase-3 (Fig. 5) suggest that HED-induced cell death includes apoptosis. The precise mechanisms regulating apoptotic events in neuronal cells remain largely unclear; however, high levels of ROS generation and the increases in the mitochondrial permeability appear to be common occurrences in many forms of apoptotic neuronal cell death. The finding that HED induced a significant ROS generation and that *N*-acetyl-L-cysteine pretreatment clearly blocked the apoptosis suggests that ROS generation is an essential trigger for HED-induced apoptosis in the SH-SY5Y cells. The source of ROS generation has not been identified; however, the catechol ring is kept in the structure of HED like dopamine and 6-OHDA; therefore, the catechol oxidation might be one of the

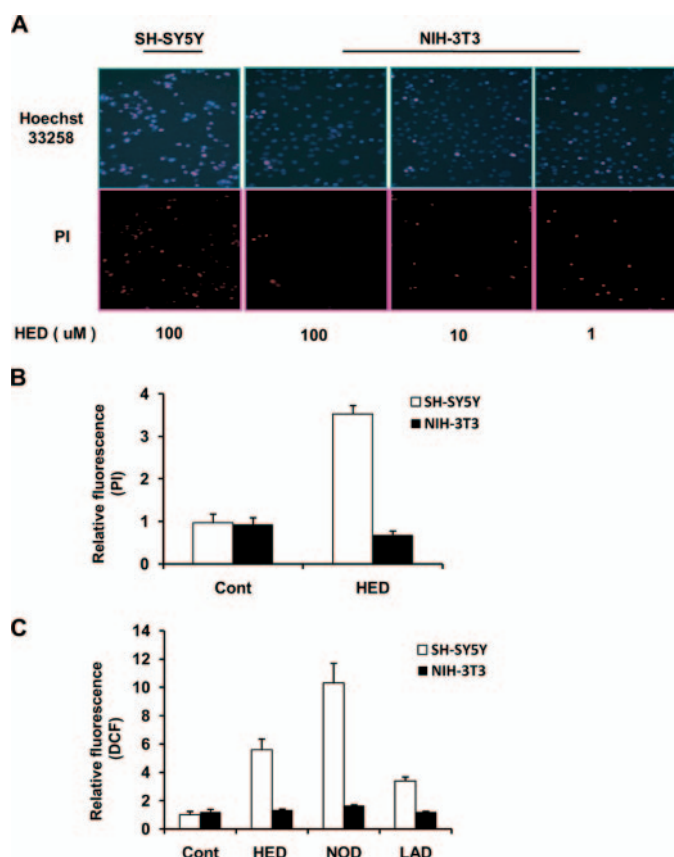


**FIGURE 8. No cytotoxicity was induced by HED in NIH3T3 cells compared with in SH-SY5Y cells.** A, apoptotic cells imaging. NIH3T3 cells were treated with different concentrations of HED for 12 h. PI and Hoechst staining were performed by fluorescence microscope. B, numbers of apoptotic cells. The apoptotic cells were analyzed by PI staining by using a flow cytometer. C, ROS generation. The fluorescence of DCF was measured by flow cytometer. The data are shown in B and C as the means  $\pm$  S.D. ( $n = 3$ ). Cont, control.

important causes for ROS generation in the HED-treated SH-SY5Y cells. The regulation of neuronal apoptosis is generally characterized by several signaling mediators such as p53, Bcl-2 family proteins, and cytochrome *c* release (54). A significant release of cytochrome *c* from mitochondrial fraction in HED-treated SH-SY5Y cells was found (Fig. 6), suggesting that the apoptosis may be critically mediated via a mitochondrial abnormality; however, the changes of Bcl-2, Bax, and phosphorylated p53 expression were not seen (data not shown); therefore, the upstream regulators of mitochondrial abnormality remain to be elucidated in further studies.

Monoamine transporters are of fundamental importance for proper signaling between neurons. Plasma membrane transporters, the major subclass of intracellular transporters (55), include the DAT, NET, and 5-HTT. In this study, pretreatment with inhibitors of DAT, NET, and 5-HTT significantly suppressed ROS generation and apoptosis events induced by HED (Fig. 7). In the case of 6-OHDA, similar to HED, a high affinity for several catecholaminergic plasma membrane transporters, such as DAT and NET, is also essential for its entrance into the neuronal cells to inflict damage. The dependence of monoamine transporter is considered to be due to a structural similarity between the monoamine transporter and dopamine and norepinephrine. The necessity of the monoamine transporter in HED-

induced cytotoxicity was further demonstrated by the result that HED could not induce apoptotic cell death and ROS generation in the monoamine transporter-absent NIH-3T3 cells (Fig. 8), which also indicates that HED may selectively induce cytotoxicity in different cell lines.

PRD, HED, NOD, and LAD, which have 3, 6, 9, and 12 of carbons in the methyl terminus based on the dopamine structure, respectively, caused apparent cell death and ROS generation in SH-SY5Y cells in the order of PRD < HED  $\approx$  NOD  $\approx$  LAD (Figs. 4B and 7B), which suggests that the specific carbon number in the C terminus might be required for the dopamine adduct-induced cytotoxicity. On the other hand, SUD and GLD, which are C terminus adducts, showed no toxicity to the SH-SY5Y cells. Moreover, to further confirm the difference of the cytotoxicity between the C terminus and the C terminus in dopamine adducts, we synthesized a compound named hexanoyl dihydroxyphenylalanine (HEDOPA), which structurally distinguishes HED as HEDOPA that possesses a more C terminus than HED, by the reaction of hexanoyl acid with dihydroxyphenylalanine (L-DOPA), which is the precursor of dopamine. Following HEDOPA treatment in the SH-SY5Y cells compared with HED, HEDOPA did not alter the viability and induce ROS generation in the cells (data not shown). These results reveal that the C terminus may structurally inhibit the transport of dopamine adducts into the cells and subsequently block the induction of cytotoxicity.

The formation of the dopamine adducts in the study are established by free polyunsaturated acid. In fact, either DHA or AA is located almost exclusively in the SN2 position of phosphoglycerides found in the neural cell membranes (56, 57); however, free fatty acid levels are reported to increase with aging because of an increasing degradation by phospholipase A<sub>2</sub> (58–60), which selectively acts on phosphoglycerides (61). DHA is the most enriched polyunsaturated fatty acid in the brain, and it has been implicated that DHA concentration is decreased in Alzheimer disease brain (62); hence, the DHA-derived dopamine adducts formed in this study may be useful biomarkers for not only PD but also Alzheimer disease.

In summary, we synthesized four dopamine adducts derived from DHA and AA and revealed the *in vivo* formation during the reaction of lipid hydroperoxides with dopamine. We observed HED, an AA-derived dopamine adduct, as a potent neurotoxin based on the significant induction of ROS generation and apoptosis in human neuroblastoma SH-SY5Y cells. The mechanism of HED-induced apoptosis has not been fully established in this study; however, it seems to be mediated by ROS generation, mitochondrial abnormalities, and monoamine transporter. The HED-induced cytotoxicity is confirmed by an *in vitro* experimental system in this study, and further studies showing the existence and the cytotoxicity in human subjects are needed.

**Acknowledgments**—We gratefully thank Dr. Takahiro Shibata (Nagoya University, Japan) for valuable advice and discussions. We also gratefully thank Dr. Komron S. Rahgozar (Stanford University Medical School) for critical and careful reading and editing of the manuscript.



## REFERENCES

- Galvan, A., and Wichmann, T. (2008) *Clin. Neurophysiol.* **119**, 1459–1474
- Fahn, S., and Cohen, G. (1992) *Ann. Neurol.* **32**, 804–812
- Leroy, E., Boyer, R., Auburger, G., Leube, B., Ulm, G., Mezey, E., Harta, G., Brownstein, M. J., Jonnalagada, S., Chernova, T., Dehejia, A., Lavedan, C., Gasser, T., Steinbach, P. J., Wilkinson, K. D., and Polymeropoulos, M. H. (1998) *Nature* **395**, 451–452
- Schapiro, A. H. (2001) *Adv. Neurol.* **86**, 155–162
- Balaban, R. S., Nemoto, S., and Finkel, T. (2005) *Cell* **120**, 483–495
- Jenner, P. (2003) *Ann. Neurol.* **53**, S26–S38
- Porter, N. A., Caldwell, S. E., and Mills, K. A. (1995) *Lipids* **30**, 277–290
- Simopoulos, A. P. (1999) *Am. J. Clin. Nutr.* **70**, 560–569
- Hadders-Algra, M. (2008) *J. Perinat. Med.* **36**, 101–109
- Kato, Y., Makino, Y., and Osawa, T. (1997) *J. Lipid Res.* **38**, 1334–1346
- Kato, Y., and Osawa, T. (1998) *Arch. Biochem. Biophys.* **351**, 106–114
- Kato, Y., Mori, Y., Makino, Y., Morimitsu, Y., Hiroi, S., Ishikawa, T., and Osawa, T. 1999 *J. Biol. Chem.* **274**, 20406–20414
- Kawai, Y., Kato, Y., Fujii, H., Mkino, Y., Mori, Y., Naito, N., and Osawa, T. (2003) *J. Lipid Res.* **44**, 1124–1131
- Kawai, Y., Fujii, H., Kato, Y., Kodama, M., Naito, N., Uchida, K., and Osawa, T. (2004) *Biochem. Biophys. Res. Commun.* **313**, 271–276
- Kawai, Y., Fujii, H., Okada, M., Tsuchie, Y., Uchida, K., and Osawa, T. (2006) *J. Lipid Res.* **47**, 1386–1398
- Bove, J., Prou, D., Perier, C., and Przedborski, S. (2005) *NeuroRx* **2**, 484–494
- Gotz, M. E., Kunig, G., Riederer, P., and Youdim, M. B. (1994) *Pharmacol. Ther.* **63**, 37–122
- Hald, A., and Lotharius, J. (2005) *Exp. Neurol.* **193**, 279–290
- LaVoie, M. J., and Hastings, T. G. (1999) *J. Neurochem.* **73**, 2546–2554
- Tapiero, H., Ba, G. N., Couvreur, P., and Tew, K. D. (2002) *Biomed. Pharmacother.* **56**, 215–222
- Lin, M. T., and Flint, B. M. (2006) *Nature* **433**, 787–795
- Wakamatsu, K., Fujikawa, K., Zucca, F. A., Zecca, L., and Ito, S. (2003) *J. Neurochem.* **86**, 1015–1023
- Graumann, R., Paris, I., Martinez-Alvarado, P., Rumanque, P., Perez-Pastene, C., Cardenas, S. P., Marin, P., Diaz-Grez, F., Caviedes, R., Caviedes, P., and Segura-Aguilar, J. (2002) *Pol. J. Pharmacol.* **54**, 573–579
- Saner, A., and Thoenen, H. (1971) *Mol. Pharmacol.* **7**, 147–154
- Pezzella, A., d'Ischia, M., Napolitano, A., Misuraca, G., and Prota, G. (1997) *J. Med. Chem.* **40**, 2211–2216
- Izumi, Y., Sawada, H., Sakka, N., Yamamoto, N., Kume, T., Katsuki, H., Shimohama, S., and Akaie, A. (2005) *J. Neurosci. Res.* **79**, 849–860
- Maharaj, H., Mahara, D. S., Scheepers, M., Mokokong, R., and Daya, S. (2005) *Brain Res.* **1063**, 180–186
- Chinopoulos, C., and Adam-Vizi, V. (2006) *FEBS J.* **273**, 433–450
- Kluck, R. M., Bossy-Wetzel, E., Green, D. R., and Newmeyer, D. D. (1997) *Science* **275**, 1132–1136
- Kita, T., Wagner, G. C., and Nakashima, T. (2003) *J. Pharmacol. Sci.* **92**, 178–195
- Mariani, E., Polidori, M. C., Cherubini, A., and Mecocci, P. (2005) *J. Chromatogr. B* **827**, 65–75
- Liu, X. B., Shibata, T., Hisaka, S., and Osawa, T. (2008) *J. Clin. Biochem. Nutr.* **43**, 26–33
- Zecca, L., Youdim, M. B. H., Riederer, P., Connor, J. R., and Crichton, R. R. (2004) *Nat. Rev. Neurosci.* **5**, 863–873
- Shibata, T., Iio, K., Kawai, Y., Shibata, Y., Kawaguchi, M., Toi, S., Kobayashi, M., Kobayashi, M., Yamamoto, K., and Uchida, K. (2006) *J. Biol. Chem.* **281**, 1196–1204
- Siegel, S. J., Bieschke, J., Powers, E. T., and Kelly, J. W. (2007) *Biochemistry* **46**, 1503–1510
- Long, E. K., Murphy, T. C., Leipson, L. J., Watt, J., Morrow, J. D., Milne, G. L., Howard, J. R., and Picklo, M. J. Sr. (2008) *J. Neurochem.* **105**, 714–724
- Maruyama, W., and Naoi, M. (2002) *J. Neurol.* **249**, 6–10
- Shamoto-Nagai, M., Maruyama, W., Kato, Y., Isobe, K., Tanaka, M., Naoi, M., and Osawa, T. (2003) *J. Neurosci. Res.* **74**, 589–597
- Dexter, D. T., Carter, C. J., Wells, F. R., Javoy-Agid, F., Agid, Y., Lees, A., Jenner, P., and Marsden, C. D. (1989) *J. Neurochem.* **52**, 381–389
- Yoritaka, A., Hattori, N., Uchida, K., Tanaka, M., Stadtman, E. R., and Mizuno, Y. (1996) *Proc. Natl. Acad. Sci. U. S. A.* **93**, 2696–2701
- Dexter, D. T., Holley, A. E., Filtter, W. D., Slater, T. F., Wells, F. R., Daniel, S. E., Lees, A., Jenner, P., and Marsden, C. D. (1994) *Mov. Disord.* **9**, 92–97
- Buhmann, C., Arlt, S., Kontush, A., Moeller-Bertram, T., Sperber, S., Oechsner, M., Stuerenburg, H. J., and Beisiegel, U. (2004) *Neurobil. Dis.* **15**, 160–170
- Montine, K. S., Quinn, J. F., Zhang, J., Fessel, J. P., Roberts, L. J., II, Morrow, J. D., and Montine, T. J. (2004) *Chem. Phys. Lipids* **128**, 117–124
- Ang, S. L. (2006) *Development* **133**, 3499–3506
- Navarro, A., and Boveris, A. (2007) *Am. J. Physiol.* **292**, C670–C686
- Forster, M. J., Dubey, A., Dawson, K. M., Stutts, W. A., Lal, H., and Sohal, R. S. (1996) *Proc. Natl. Acad. Sci. U. S. A.* **93**, 4765–4769
- Boveris, A., and Navarro, A. (2008) *IMUBM Life* **60**, 308–314
- Asanuma, M., Miyazaki, I., and Ogawa, N. (2003) *Neurotox. Res.* **5**, 165–176
- Hanrott, K., Gudmunson, L., O'Neill, M. J., and Wonnacott, S. (2006) *J. Biol. Chem.* **281**, 5373–5382
- Chalovich, E. M., Zhu, J. H., Caltagarene, J., Bowser, R., and Chu, C. T. (2006) *J. Biol. Chem.* **281**, 17870–17881
- Jia, Z., Zhu, H., Misra, H. P., and Li, Y. (2008) *Brain Res.* **1197**, 159–169
- Lee, Y. M., Park, S. H., Shin, D. I., Hwang, J. Y., Park, B., Park, Y. J., Lee, T. H., Chae, H. Z., Jin, B. K., Oh, T. H., and Oh, Y. J. (2008) *J. Biol. Chem.* **283**, 9986–9998
- Berman, S. B., and Hastings, T. G. (1999) *J. Neurochem.* **73**, 1127–1137
- Gorman, A. M., Ceccatelli, S., and Orrenius, S. (2000) *Dev. Neurosci.* **22**, 348–358
- Gethe, U., Andersen, P. H., Larsson, O. M., and Schousboe, A. (2006) *Trends Pharmacol. Sci.* **27**, 375–383
- Ma, Q. L., Teter, B., Ubada, O. J., Morihara, T., Dhoot, D., Nyby, M. D., Tuck, M. L., Frautschy, S. A., and Cole, G. M. (2007) *J. Neurosci.* **27**, 14299–14307
- Beermann, C., Möbius, M., Winterling, N., Schmitt, J. J., and Boehm, G. (2005) *Lipids* **40**, 211–218
- Rosenberger, T. A., Villacreses, N. E., Hovda, J. T., Bosetti, F., Weerasinghe, G., Wine, R. N., Harry, G. J., and Rapoport, S. I. (2004) *J. Neurochem.* **88**, 1168–1178
- Qu, Y., Chang, L., Klaff, J., Seeman, R., Balbo, A., and Rapoport, S. I. (2003) *Brain Res. Brain Res. Protoc.* **12**, 16–25
- Rapoport, S. I. (1999) *Neurochem. Res.* **24**, 1403–1415
- Diez, E., Chilton, F. H., Stroup, G., Mayer, R. J., Winkler, J. D., and Fonteh, A. N. 1994 *Biochem. J.* **301**, 721–726
- Bazan, N. G., Palacios-Pelaez, R., and Lukiw, W. J. (2002) *Mol. Neurobiol.* **26**, 283–298

---

**Lipids and Lipoproteins: Metabolism,  
Regulation, and Signaling:  
Formation of Dopamine Adducts Derived  
from Brain Polyunsaturated Fatty Acids:  
MECHANISM FOR PARKINSON  
DISEASE**

Xuebo Liu, Naruomi Yamada, Wakako

Maruyama and Toshihiko Osawa

*J. Biol. Chem.* 2008, 283:34887-34895.

doi: 10.1074/jbc.M805682200 originally published online October 15, 2008

---

Access the most updated version of this article at doi: [10.1074/jbc.M805682200](http://www.jbc.org/10.1074/jbc.M805682200)

Find articles, minireviews, Reflections and Classics on similar topics on the [JBC Affinity Sites](http://www.jbc.org/).

Alerts:

- [When this article is cited](#)
- [When a correction for this article is posted](#)

[Click here](#) to choose from all of JBC's e-mail alerts

Supplemental material:

<http://www.jbc.org/content/suppl/2008/10/17/M805682200.DC1.html>

This article cites 62 references, 15 of which can be accessed free at  
<http://www.jbc.org/content/283/50/34887.full.html#ref-list-1>